Mechanical and Tribological Properties of Glass–Epoxy Composites with and Without Graphite Particulate Filler

B. Suresha,[1,2] G. Chandramohan,[2] N. M. Renukappa,[3] Siddaramaiah[4]

[1]*Department of Mechanical Engineering, National Institute of Engineering, Mysore 570 008, India*
[2]*Department of Mechanical Engineering, Peelamedu Samanaidu Govindasamynaidu College of Technology, Coimbatore 641 004, India*
[3]*Department of Electronics and Communication Engineering, Sri Jayachamarajendra College of Engineering, Mysore 570 006, India*
[4]*Department of Polymer Science and Technology, Sri Jayachamarajendra College of Engineering, Mysore 570 006, India*

Received 11 May 2006; accepted 24 August 2006
DOI 10.1002/app.25413
Published online in Wiley InterScience (www.interscience.wiley.com).

ABSTRACT: The objectives of this research article is to evaluate the mechanical and tribological properties of glass-fiber-reinforced epoxy (G–E) composites with and without graphite particulate filler. The laminates were fabricated by a dry hand layup technique. The mechanical properties, including tensile strength, tensile modulus, elongation at break, and surface hardness, were investigated in accordance with ASTM standards. From the experimental investigation, we found that the tensile strength and dimensional stability of the G–E composite increased with increasing graphite content. The effect of filler content (0–7.5 wt %) and sliding distance on the friction and wear behavior of the graphite-filled G–E composite systems were studied. Also, conventional weighing, determination of the coefficient of friction, and examination of the worn surface morphological features by scanning electron microscopy (SEM) were done. A marginal increase in the coefficient of friction with sliding distance for the unfilled composites was noticed, but a slight reduction was noticed for the graphite-filled composites. The 7.5% graphite-filled G–E composite showed a lower friction coefficient for the sliding distances used. The wear loss of the composites decreased with increasing weight fraction of graphite filler and increased with increasing sliding distance. Failure mechanisms of the worn surfaces of the filled composites were established with SEM. J Appl Polym Sci 103: 2472–2480, 2007

Key words: composites; failure; fillers; mechanical properties; surfaces

INTRODUCTION

Polymers and their composites find use in many engineering applications as alternative products to metal-based ones. Wide ranges of thermoplastic and thermosetting varieties of polymers are available and, in addition, offer advantages in terms of ease of fabrication. This has contributed in a big way to the advent of newer polymer composite materials that find wide application in industries for the manufacture of a wide variety of products, such as automobile components, aircraft components, structural components, and sporting goods. Some commonly used polymers include polytetraflouroethylene (PTFE), poly(ether ether ketone), vinyl ester, unsaturated polyester, epoxy, and so on. Among these, epoxies posses excellent mechanical properties and good chemical and corrosion resistance. Also, epoxies in molded or cast form have excellent dimensional stability and low shrinkage. Furthermore, easy processability by the mere addition of a curing agent with or without the application of heat places these materials above others. Furthermore, it has been reported that epoxies reinforced with fillers and fibers possess very good mechanical and tribological properties.

Automotive and aircraft components fabricated with fiber-reinforced polymeric composites (FRPCs) have tight requirements in service, and they are required to withstand mechanical damage during service. Kim et al.[1] reported that fiber damage could occur during the fabrication process, transport, storage, and maintenance. Unal and Mimaroglu[2] evaluated the mechanical properties of nylon 6 by adding one or a combination of more than one filler and by varying the weight percentage. They observed that the tensile strength and modulus of elasticity of nylon 6 composites increased with increasing filler weight percentage. Varada Rajulu et al.[3] investigated the tensile properties of epoxy toughened with hydroxyl-terminated polyester at different layers of glass roving and reported that the tensile strength increased with increasing fiber content. It is understood that the fracture performance of fiber composites is mostly dominated by the following failure mechanisms: (1) mechanisms related to the

Correspondence to: B. Suresha (sureshab2004@yahoo.co.in).

contribution of the matrix, such as matrix plastic deformation and matrix fracture; (2) mechanisms related to the interface of the matrix and fibers, mainly matrix/fiber debonding and fiber pullout; and (3) mechanisms related to fiber fracture.[4,5] The service temperature, duration, and magnitude of stress determine the failure mechanism of composite materials. Fiber reinforcement affects the strength, durability, thermal conductivity, and creep resistance of the composite and also the failure mechanism.[6]

For tribological loaded components, the coefficient of friction, mechanical load carrying capacity, and wear rate of the materials determine their acceptability for industrial applications. Polymer-based composite materials are the ones used in such tribological applications because of their ever-increasing demand in terms of stability at higher loads, temperatures, and better lubrication and wear properties.[7,8] Various researchers have studied the tribological behavior of FRPCs. Studies have been conducted with various shapes, sizes, types, and compositions of fibers in a number of matrices.[9–16] For glass-fiber-reinforcing polymer composites,[13,14] the process of material removal in dry sliding wear is dominated by matrix wear, fiber sliding wear, fiber fracture, and interfacial debonding. The last two mechanisms, fiber fracture and interfacial debonding, occur sequentially and can be considered a combined process. Polymers reinforced with glass fibers[15] have a higher wear rate than the same polymers reinforced with carbon fibers. This depends partly on the lubricating properties of the carbon fibers and partly on the high abrasiveness of glass fiber particles. Tanaka et al.[16] studied the wear behavior of glass-fiber-reinforced, carbon-fiber-reinforced, and carbon-bead-reinforced PTFE. The glass-fiber-reinforced PTFE showed a very low wear rate with a steel countersurface. It was also reported that the fiber preferentially supported the applied load, and a fiber rich layer was produced during rubbing on the mating surface. In general, these materials exhibit an improvement in wear and friction resistance compared to pure unfilled polymers. An understanding of the friction and wear mechanisms of polymers would aid in the development of composites for the solution of technological problems. It was previously reported[17,18] that the friction and wear behavior of FRPCs exhibits anisotropic characteristics.

The modification of the tribological behavior of fiber-reinforced polymers by the addition of filler material was reported[19] to be quite encouraging. Most studies on filler action in the case of polymer composites sliding against metallic counterfaces have focused on the reduction of wear rate and the coefficient of friction. In addition to the higher mechanical strength obtained because of the addition of fillers in polymeric composites, there is a direct cost reduction due to the lower consumption of resin material. The critical and final selection of filler primarily depends on the requirements of the end product, the interface compatibility, and the dimension/shape of the particles. Various researchers[20–25] have reported that the wear resistance of polymers was improved by the addition of fillers. Some of the fillers that are effective in reducing friction and wear are MoS_2, CuO, CuS, and Al_2O_3. Kishore et al.[25] analyzed the influence of sliding speed and load on the friction and wear behavior of glass-reinforced polymer composites filled with either rubber or oxide particles; they reported that the wear loss increased with increasing load/speed. The use of graphite as a filler material is known to improve the mechanical and tribological properties of metal matrix composites.[26]

Most of the previous findings were based on either randomly oriented or unidirectionally oriented fiber composites. Woven-fabric-reinforced composites are gaining popularity because of their balanced properties in the fabric plane and their ease of handling during fabrication. Mody et al.[27] showed that the simultaneous existence of parallel and perpendicular oriented carbon fibers in a woven configuration led to a synergistic effect on the enhancement of the wear resistance of the composite. Hence, in this research study, we took up E-glass woven-fabric-reinforced epoxy composites with powdered graphite as a filler material for investigation with the intention of characterizing them for their mechanical properties, friction, and dry slide wear behavior.

EXPERIMENTAL

Materials

Woven glass fabrics (360 g/m^2) containing E-glass fibers with diameters of 5–12 μm were used. The matrix system was a medium-viscosity (3000 MN/m^2; density = 1.16 g/cc) epoxy resin (LAPOX L-12) and a room-temperature curing polyamine hardener (K-6); both were supplied by ATUL India, Ltd. (Gujarat, India). The filler material was graphite powder with particle sizes in the range 50–60 μm, which was procured from a local market.

Manufacturing of the composites and preparation of the test samples

E-glass plain-weave woven roving fabric, which was compatible with epoxy resin, was used as the reinforcement. The epoxy resin was mixed with the hardener in the ratio 100:12 w/w. A dry hand layup technique was used to produce the composites. The stacking procedure consisted of the placement of the fabric, one above the other, with the resin mix well spread between the fabrics. A porous Teflon film was placed

TABLE I
Details of the Prepared Test Samples

Sample code	Matrix	Reinforcement	Graphite (wt %)
A	Epoxy	E-glass fabric	0.0
B	Epoxy	E-glass fabric	2.5
C	Epoxy	E-glass fabric	5.0
D	Epoxy	E-glass fabric	7.5

on the completed stack. To ensure uniform thickness of the sample, a 3 mm spacer was used. The mold plates were coated with release agent to prevent damage to the solidified panel on separation. The whole assembly was kept in a hydraulic press (0.5 MPa) and allowed to cure for a day at room temperature. The panel so prepared had a size 250 mm × 250 mm × 3 mm. To prepare the graphite-filled glass-fiber-reinforced epoxy (G–E) composites, graphite powder was mixed with a known amount of the epoxy resin. The details of the composites are shown in Table I. The test samples were cut with the help of a diamond-tipped cutter as per ASTM standards.

Mechanical and slide wear test methods

The mechanical properties, including tensile strength, tensile modulus, and elongation at break, were investigated with a J. J. Lloyd universal testing machine (1–20 kN, London, UK) in accordance with ASTM D 638. When the tensile strength test was conducted, a crosshead speed of 5 mm/min was maintained. Five samples were tested for each combination of the composites. The hardness of the unfilled and graphite-filled G–E samples were measured with a Rockwell hardness tester (Rockwell C; Newage testing instruments, Inc., Southampton).

A pin-on-disc setup was used for slide wear experiments. The surface (5 mm × 5 mm), glued to a pin with a diameter of 6 mm and a length of 22 mm, came in contact with a hardened disc with a hardness of 62 HRc. It was made of En 32 steel with a diameter of 160 mm, a thickness of 8 mm, and a surface roughness of 0.84 μm. The test was conducted on a track with a diameter of 115 mm by selection of the test duration, load, and velocity in accordance with ASTM G-99. Before testing, the test samples were polished against 600-grade SiC paper to ensure proper contact with the countersurface. The surfaces of both the sample and the disc were cleaned with a soft paper soaked in acetone and were thoroughly dried before the test. The pin assembly was initially weighed to an accuracy of 0.0001 g in a digital electronic balance. The test was carried out by application of a load of 40 N at a constant sliding velocity of 4 m/s for different sliding distances (500–6000 m). The difference between the initial and final weights was a measure of slide wear loss. For each condition, at least three tests were performed, and the mean value of weight loss was reported. A 20-kg load cell was fixed tangential to the lever arm, through which the friction force was measured.

For selected combinations of load and sliding velocity, the samples were sputter-coated with gold for detailed morphological behavior with a Leica scanning electron microscope (XL30 SEM with an Oxford ISIS310 EDX, Cambridge, England).

RESULTS AND DISCUSSION

Mechanical properties

The measured tensile behavior and surface hardness test results of the unfilled and graphite-filled G–E composites are shown in Table II. If the results are compared, one can see that the 7.5 wt % graphite-filled G–E sample showed the highest tensile strength value, which confirmed the effect of the incorporation of graphite filler, which improved the fiber–matrix interface in the composite. This was attributed to the fact that in the absence of graphite, the failure propagated along the loading direction. The addition of graphite particles caused a dispersion of these particles in the matrix, which impeded the propagation of failure along the loading direction. The failure, therefore, propagated in a direction dictated by the dispersoid concentration in the matrix. This means that the failure propagated easily in the directions where the dispersoid concentration was lower, which led to an increased tensile strength, increased tensile modulus, lower elongation, and increased surface hardness and, thus, better dimen-

TABLE II
Mechanical Properties of the G–E and Graphite-Filled G–E Samples

Property	Sample code			
	A	B	C	D
Tensile strength (MPa)	164.51 ± 16	182.6 ± 12	191.0 ± 13	205.1 ± 10
Tensile modulus (MPa)	8,558 ± 70	9,857 ± 54	10,006 ± 49	10,501 ± 45
Elongation (%)	3.85 ± 0.15	3.49 ± 0.10	3.39 ± 0.10	3.30 ± 0.12
Hardness (Rockwell C)	102 ± 5	110 ± 5	112 ± 4	118 ± 3

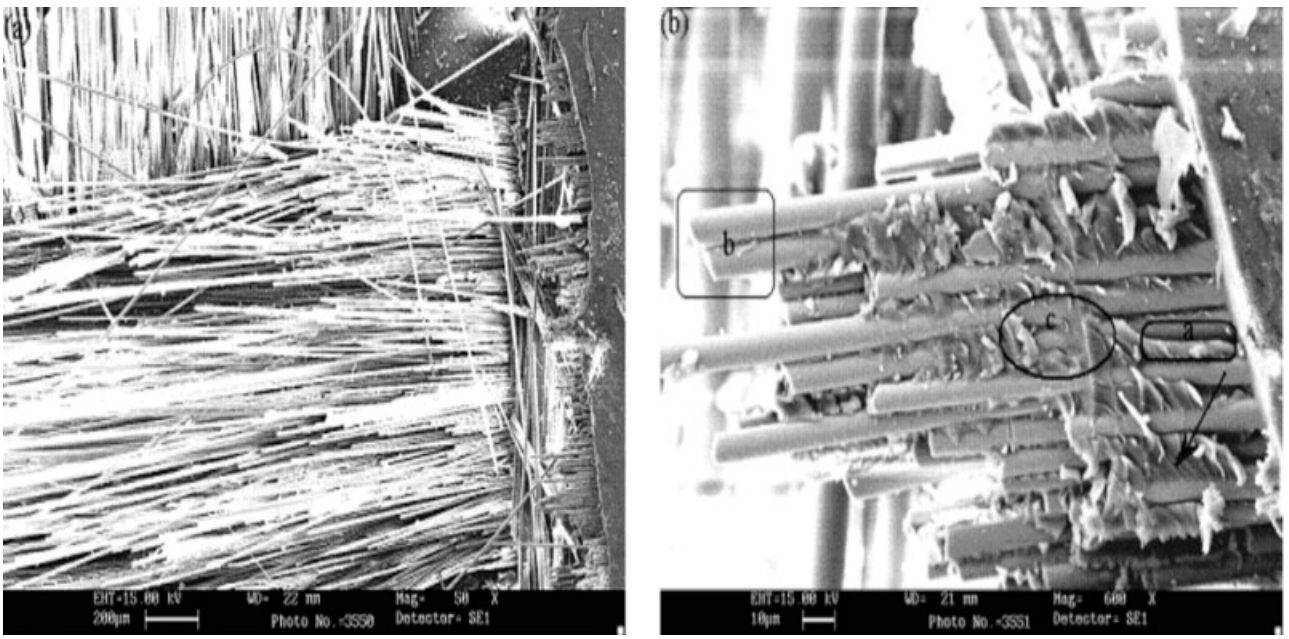

Figure 1 SEM photomicrographs of sample A after tensile testing at (a) 50× and (b) 600× magnification.

sional stability. Also, the tensile strength of the filled G–E samples increased with increasing graphite content. In tensile strength tests, the fibers in a composite fail at different stress levels as the applied tensile load increases. Some main failure modes in tensile testing are cited in the literature.[28,29] In this study, the unfilled composite showed the lowest tensile strength values, and the main failure mode was fiber–matrix debonding. In this case, cracks at different cross-sections of the specimen joined together to cause fiber–matrix debonding or shear failure of the matrix. These types of matrix shear failures and fiber–matrix debonding occurred either independently or in combination. Master[29] observed similar failure mechanisms for continuous fiber composites.

The surface hardness of filled G–E samples increased with increasing graphite content (Table II). The higher the proportion of graphite was, the greater the Rockwell hardness of the G–E sample was; that was in the range 102–118. The reduction in percentage elongation at break of the composite was noticed with increasing filler content as expected.

Fracture analysis

The scanning electron microscopy (SEM) micrographs in Figures 1(a,b) and 2(a,b) show the fractured surfaces of the unfilled and graphite-filled G–E composite systems, respectively. The microphotographs revealed linear elastic behavior and brittle-type fracture for the test samples, along with instant multiple fractures. The fracture was due to delamination between the layers of the composite samples and fiber pullout [Fig. 1(a)]. As shown in Table II, with increasing graphite percentage, the percentage elongation showed a clear decreasing trend. Although no chemical reaction was possible, some physical interaction had to be considered. Interestingly, the composite characterized by a higher tensile strength showed brittle fractures. For sample A, the fracture was brittle and could be explained by the plastic deformation of the matrix after fiber–matrix debonding. The SEM micrograph shown in Figure 1(b) supported this failure mechanism because the fibers on the fractured surfaces were clean; this showed brittle fracture. Other important failure mechanisms of the composites, such as fiber fracture (marked b), cohesive resin fracture (marked c), and fiber–matrix debonding (marked a) were also observed in the SEM micrograph [Fig. 1(b)]. Generally, matrix fracture initiated at the surface of the fibers, as indicated by the direction of river lines (marked by an arrow) and propagated into the resin on either side, where cracks extended from the surfaces of adjacent fibers simultaneously.

SEM micrographs of the graphite-filled G–E fractured surface samples in tension revealed very different fracture morphologies [Fig. 2(a)] than that of the unfilled G–E sample; graphite-filled G–E composites revealed the simultaneous breakage of fibers and matrix, which evidenced better interfacial adhesion [marked A in Fig. 2(a)] and led to a higher tensile strength. The granular appearance of the matrix surface was attributed to the uniform distribution of the graphite filler. These gave rise to clus-

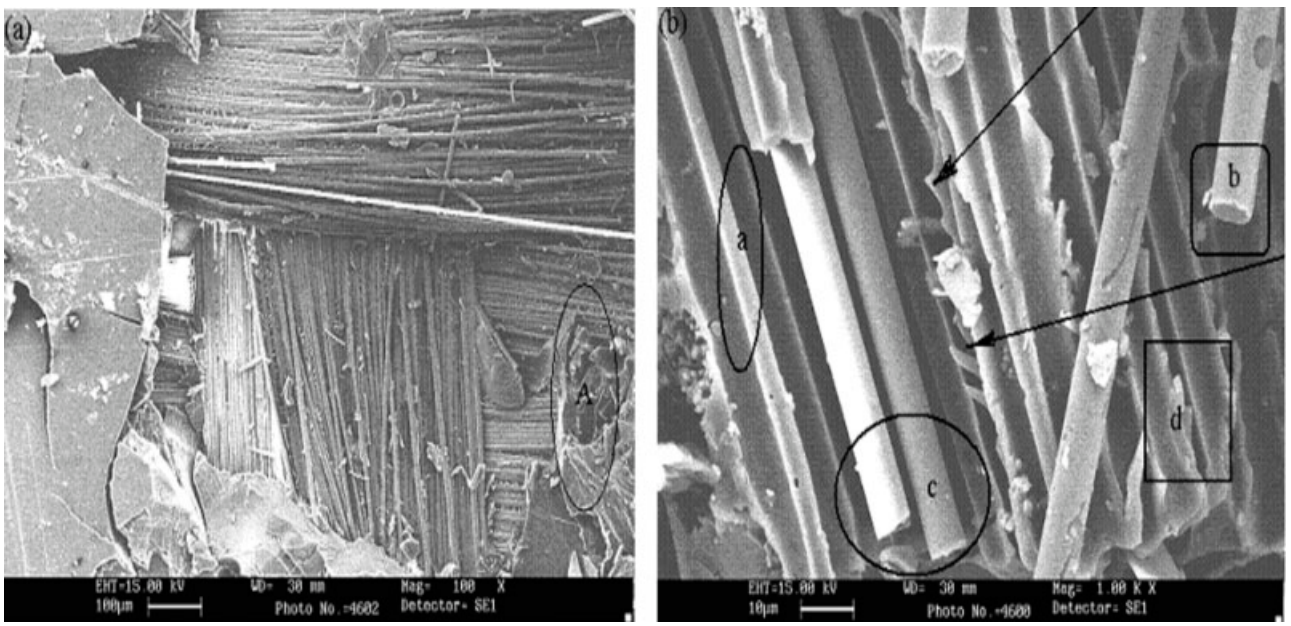

Figure 2 SEM photomicrographs of sample D after tensile testing at (a) 100× and (b) 1000× magnification.

tering, which tended to align in clumps in the direction of the fracture. Because peeling was not symmetrical, localized shear stresses may have been introduced into the failures as a consequence of strain difference between the fibers, which resulted in the formation of shallow cusps [marked by arrows in Fig. 2(b)]. Other important failure features, such as a ridge in the matrix (marked a), a radial pattern on the fiber (marked b), fiber fracture (marked c), fiber–matrix debonding (marked d), and graphite particles adhering to the surface of the fiber, and good fiber–matrix bonding are also evident in the SEM micrograph [Fig. 2(b)].

Friction and wear results

The results of the coefficient of friction and wear loss as a function of sliding distance at a load of 40 N and a sliding velocity of 4 m/s are shown in Figures 3 and 4, respectively. As shown in these figures, there was a strong interdependence on the friction coefficient and wear loss with respect to

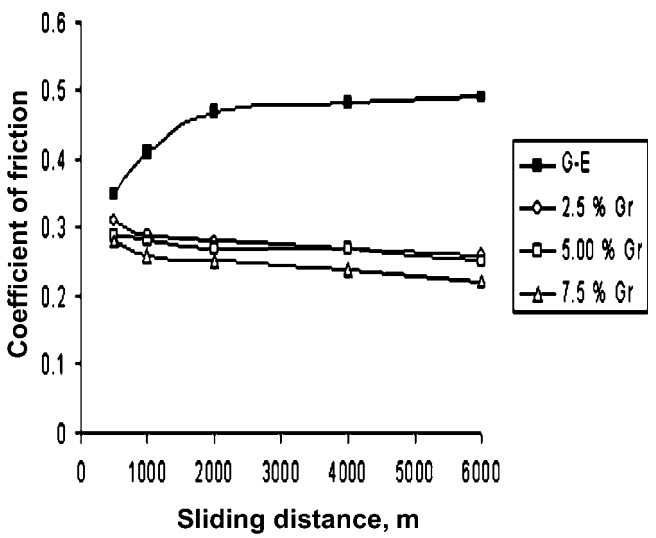

Figure 3 Coefficient of friction versus sliding distance at a load of 40 N and a sliding velocity of 4 m/s. %GR: percent graphite.

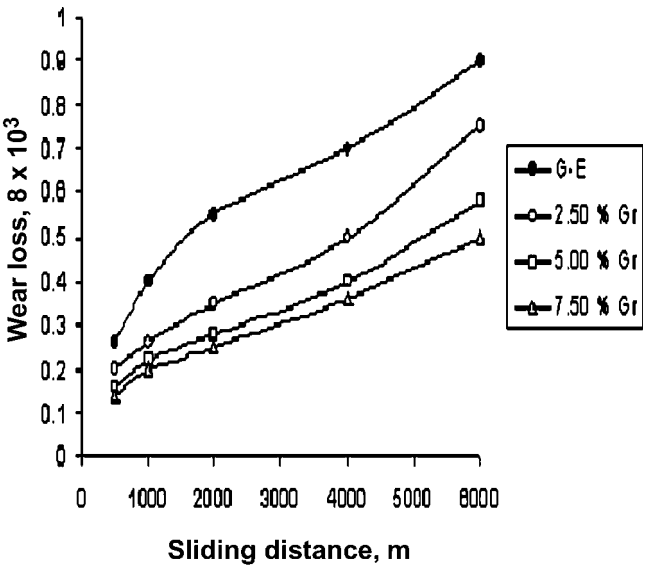

Figure 4 Wear loss verse sliding distance at a load of 40 N and a sliding velocity of 4 m/s. %GR: percent graphite.

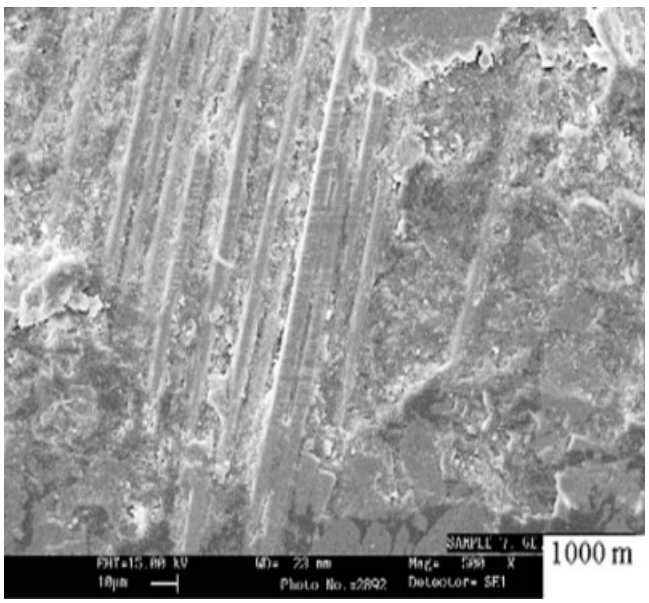

Figure 5 SEM photomicrographs of sample A at a sliding distance of 1000 m.

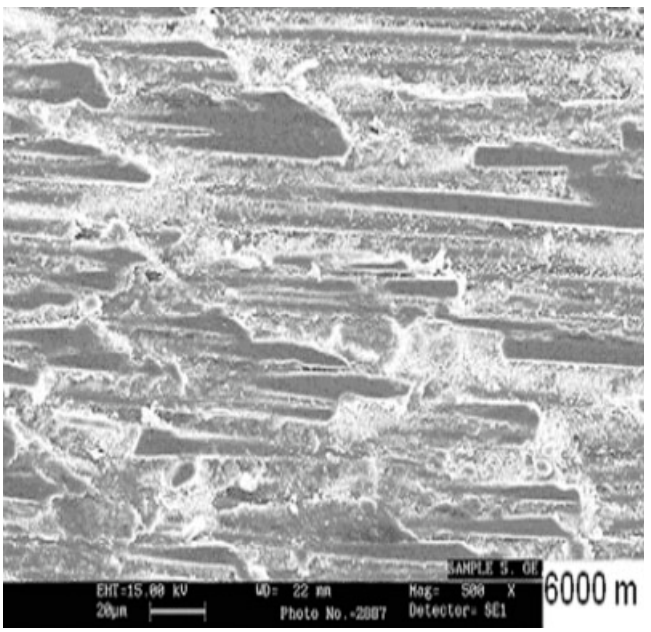

Figure 7 SEM photomicrographs of sample A at a sliding distance of 6000 m.

the sliding distance. The representative SEM photographs of the composite samples after wear testing are shown in Figures 5–10.

Coefficient of friction

The variation in the coefficient of friction with sliding distance for a constant sliding velocity of 4 m/s is shown in Figure 3, where the fluctuations in the coefficient of friction were scattered within ±20% of the mean; only the mean values are plotted here. As shown in Figure 3, the coefficient of friction of the filled G–E composites was lower than that of the unfilled G–E composite, which varied between 0.22 to 0.31. Also, the coefficient of friction of sample A increased with increasing sliding distance up to 2000 m and reached a steady-state condition after a sliding distance of 2000 m. During this transient period, a number of phenomena occurred, including

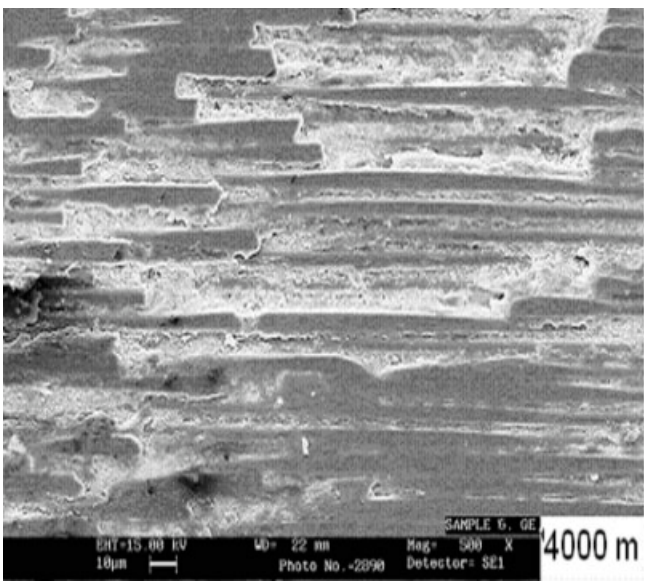

Figure 6 SEM photomicrographs of sample A at a sliding distance of 4000 m.

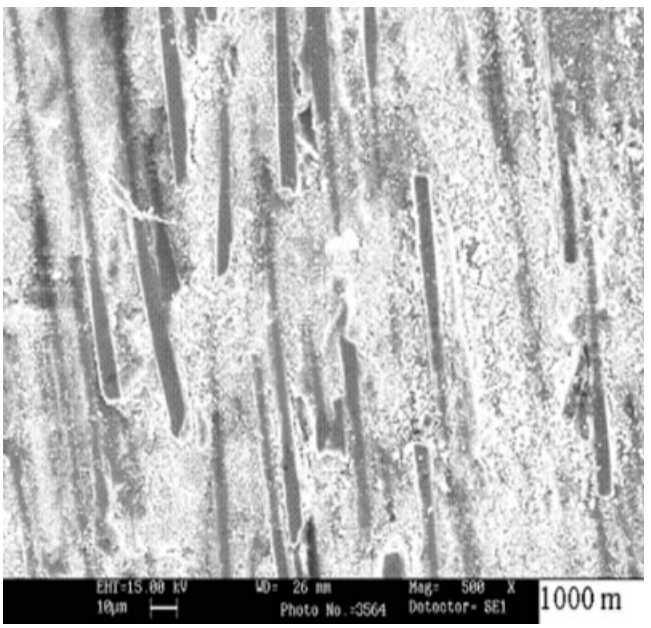

Figure 8 SEM photomicrographs of sample D at a sliding distance of 1000 m.

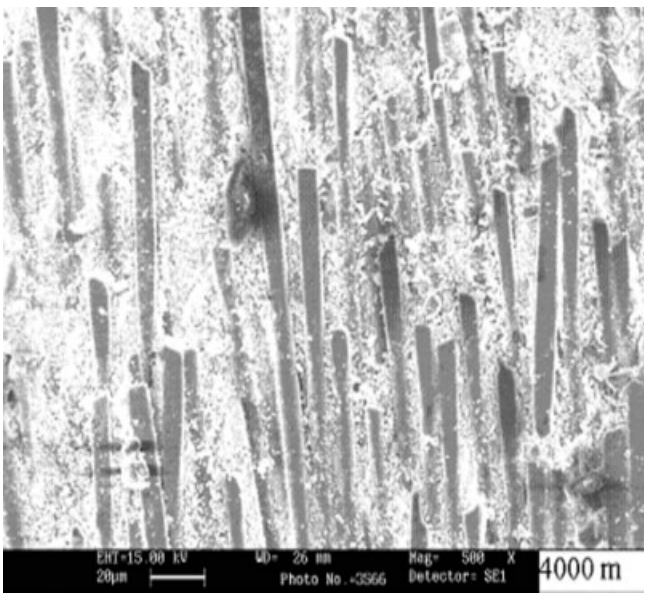

Figure 9 SEM photomicrographs of sample D at a sliding distance of 4000 m.

changes in the countersurface topography and the composite rubbing surface and an increase in interface temperature. In the G–E composite, the friction of the composite material seemed to be governed by its shear strength, which influenced the rupture of adhesive bonds at the interface. The likelihood of the fiber–glass disrupting the transfer film could have also been a reason for this increased friction.

However, for the graphite-filled G–E composites, the coefficient of friction decreased with increasing filler content and was almost linear. The decrease in the coefficient of friction of the graphite-filled G–E composite was attributed to the fragmentation of graphite particles and/or the dispersion of agglomerated graphite, which gave rise to a lubrication effect. There was no marked change in the coefficient of friction for 2.5 and 5.0 wt % graphite-filled composites, but there was a marginal reduction in the coefficient of friction for 7.5 wt % graphite. The effect of sliding distance on the coefficient of friction was lower for graphite-filled composites than for the unfilled composite. The maximum wear resistance and minimum friction values was achieved with 7.5 wt % graphite; this was because the lower particle size (50–60 μm) filler was uniformly distributed on the surface of the composites; this also acted as a self-lubricating agent.

Wear loss

The plot of wear loss as a function of sliding distance for G–E composites filled with different weight percentages of graphite is shown in Figure 4. As shown in the plot, the wear loss increased with increasing sliding distance for all composites. The order of wear resistance behavior of the composites was as follows: 7.5 > 5 > 2.5 > 0 wt % graphite. It was obvious from the wear data (Fig. 4) that the wear loss of sample A was higher up to 2000 m and increased gradually until 6000 m was reached. However, for the graphite-filled G–E composites, the wear loss increased almost linearly up to 4000 m, and a higher wear loss was observed between sliding distances of 4000 and 6000 m. Also, the wear resistance of graphite-filled G–E was high compared to that of the unfilled G–E composites. This behavior was in agreement with that of the tensile strength results listed in Table II.

A brief discussion of atomic structure of graphite will enhance understanding of how graphite improves the tribological properties of the polymer composites. In graphite, the carbon atoms are arranged hexagonally in a planar condensed ring. Also, the layers are stacked parallel to each other, with the atoms within the rings bonded covalently, whereas the layers are loosely bonded together by Van der Waal's forces. The anisotropic nature of graphite is the result of the two types of bonding acting in different crystallographic directions. The ability of graphite to form a solid film lubricant may be attributed to these two contrasting chemical bonds. Also, the weak Van der Waal's forces govern the bonding between the individual layers, permitting the layers to slide over one another, making it an ideal lubricant, and resulting in a reduced coefficient of friction and, hence, wear.

For the G–E composites, wear debris consists of a shear deformed polymer matrix containing broken

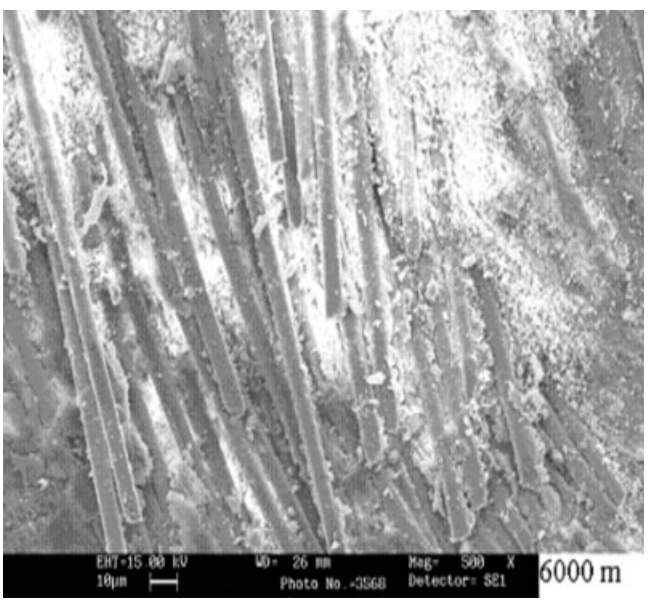

Figure 10 SEM photomicrographs of sample D at a sliding distance of 6000 m.

pulverized glass particles and a wear powder of the metallic countersurface. The particles can either be lost from the contact zone or remain there for a fixed time as a transfer layer. In such cases, their polymer component can cushion the countersurface asperities and reduce the effective toughness, but the pulverized glass component in this debris can act as a third body abrasive, which leads to an enhanced roughening of the countersurface. The friction coefficient of the G–E composite thus depended on various particles in the wear debris. Because of this, the coefficient of friction was high and so was wear.

The wear loss was low for graphite-filled G–E compared to the unfilled G–E samples. At the start of sliding, all of the asperities of the two surfaces were in contact with each other. As shear forces were applied, the asperities deformed. The graphite particles protruded out from the surface of the sample. At first, the epoxy matrix wore, and only bidirectional glass fibers were in contact with the countersurface. As sliding distance increased, the wear rate decreased. The glass fibers wore the steel countersurface. Glass fibers that were parallel to the sliding direction wore, which resulted in the thinning of fibers and subsequent breakage. Because of the high hardness of the countersurface, the glass fibers adhered to the matrix, and the adjacent fibers resisted the movement of the glass fibers into the matrix. Hence, as the sliding distance increased, the glass fibers were crushed. The broken fibers wore the sample further. The loosened particles caused third-body abrasion. When the epoxy came in contact, adhesive wear occurred, and the wear rate increased. The wear rate increased at a faster rate beyond the sliding distance of 4000 m. The mechanism controlling the wear process was delamination. Better wear resistance was obtained by the addition of graphite filler. During sliding, the graphite particles got smeared at the interface and formed a graphite film that reduced the coefficient of friction and, hence, wear.

SEM

The SEM features of sample A subjected to different sliding distances are displayed in Figures 5–7. Figure 5 shows the wear surface features corresponding to the low sliding distance of 1000 m. The worn surface showed less wear of the matrix, fewer cracks in the matrix, less retention of matrix adherence to fibers, and very few broken fibers, as shown in Figure 5. With increased sliding distance from 1000 to 4000 m, the matrix wear was higher, less debris was formed, more fiber was exposed, and there was little breakage of fibers (Fig. 6). The SEM features pertaining to a sliding distance of 6000 m are shown in Figure 7; this figure reveals that the matrix was well spread and yielded more glass fiber breakages compared to lower sliding distance conditions. Furthermore, the wear debris was uniformly distributed. These SEM features corroborated the wear data shown in Figure 4.

The influence of sliding distance on wear behavior of the graphite-filled G–E composites (7.5 wt %, sample D) was analyzed by SEM (Figs. 8–10). Figure 8 pertains to the sliding distance of the 1000-m run, which showed the wear of matrix and debris formation. Also, the debris masked the fibers. An increased sliding distance from 1000 to 4000 m showed (Fig. 9) increased debris formation and fiber breakage followed by interface separation, which thus, contributed to a higher wear loss. Furthermore, with an increase in the sliding distance to 6000 m, there was more debris concentrated on the top right corner of the microphotograph, broken fibers in large numbers, and disorientation of fibers, as shown in the SEM microphotograph in Figure 10.

CONCLUSIONS

The following are the key points that emerged from this investigation:

- This study pointed to the fact that on introduction of the graphite filler in the G–E composites, there was an improvement in the mechanical properties; this emphasized the importance of filler performance to the G–E composites. SEM observations shed further light on features such as matrix fracture, inclined fiber fracture, and disorientation of transverse fibers. When the tensile test results and morphological behavior of the tensile fractured surface of the graphite-filled G–E composites were correlated, it was revealed that a strong interface between the fiber and matrix and uniform distribution of graphite filler led to improved tensile properties.
- An increase in sliding distance led to increased slide wear loss for the composite test specimens. However, the change in the coefficient of friction with sliding distance did not obey a fixed pattern for the graphite-filled G–E composites.
- At a higher sliding distance, the abrasive wear mechanisms could govern the interaction between the surfaces in contact; in this condition, the wear resistance of the G–E composites were increased by the filling of the matrix with graphite powder. In particular, from the tests conducted in this study, the friction and slide wear behavior of 7.5 wt % graphite-filled G–E composites were better than those of the G–E composites with lower graphite filler content.
- These experimental results indicate that in the context of application as a bearing material (journal bearings and antifriction bearings), the

performance of graphite-filled G–E composite is good and possibly superior to G–E composites.

The authors are grateful to Additional Director S. Seetharamu of the Central Power Research Institute, Materials Testing Division, Bangalore, for allowing them to use the laboratory facilities for this study. They also thank P. Sampath Kumaran and Vartha Venkateswarlu for their help in taking SEM photographs and conducting experiments. The authors are also thankful to the Central Power Research Institute management for the permission extended to publish this article.

References

1. Kim, J.; Shioya, M.; Kobayashi, H.; Kaneko, J.; Kido, M. Compos Sci Technol 2004, 64, 2221.
2. Unal, H.; Mimaroglu, A. J Reinforced Plast Compos 2004, 23, 461.
3. Varada Rajulu, A.; Sanjeev Kumar, S. V.; Babu Rao, G.; Shashidhara, G. M.; He, J.; Zhang, J. J Reinforced Plast Compos 2002, 21, 1591.
4. Friedrich, K. Compos Sci Technol 1985, 22, 43.
5. Friedrich, K. In Application of Fracture Mechanics of Composite Materials; Friedrich, K., Ed.; 1989; Chapter 11, p 425.
6. Karger-Kocsis, J. In Application of Fracture Mechanics of Composite Materials; Friedrich, K., Ed.; Elsevier: New York, 1989; Chapter 6, p 189.
7. Lee, H.; Nevilee, K. Hand Book of Epoxy Resins; McGraw-Hill: New York, 1976; p 1.
8. Friedrich, K. In Friction and Wear of Polymer Composites; Friedrich, K., Ed.; Composite Material Science Series; Elsevier: Amsterdam, 1986; Vol. 1, p 233.
9. Bijwe, J.; Tewari, U. S.; Vasudevan, P. Wear 1989, 132, 247.
10. Tripaty, B. S.; Furey, M. J. Wear 1993, 162–164, 385.
11. Pihtili, H.; Tosun, N. Wear 2002, 252, 979.
12. Viswanth, B.; Verma, A. P.; Rao, C. V. S. K. Wear 1991, 145, 315.
13. Friedrich, K. Friction and Wear of Polymer Composites; Elsevier: Amsterdam, 1986.
14. Cirino, M.; Friedrich, K.; Pipes, R. B. Wear 1988, 121, 127.
15. Sung, N. H.; Suh, N. P. Wear 1979, 53, 129.
16. Tanaka, K.; Uchyama, Y.; Ueda, S.; Shimizu. In Proceedings of the JSLE-ASLE International Lubrication Conference; Sakurai, T., Ed.; Elsevier Science Publisher: Tokyo, Japan, 1975.
17. EI-Sayed, A. A.; EI-Sherbiny, M. J.; Abo-EI-Ezz, A. S.; Aggag, G. A. Wear 1995, 184, 45.
18. Kukureka, S. N.; Hooke, C. J.; Rao, M.; Liiao, P.; Chen, Y. K. Tribology Int 1999, 32, 107.
19. Briscoe, B. J.; Pogosion, A. K.; Tabor, D. Wear 1974, 27, 19.
20. Tanaka, K. In Friction and Wear of Polymer Composites; Friedrich, K., Ed.; Elsevier: Amsterdam, 1986; Vol. 205, p 137.
21. Bahadur, S.; Fu, Q.; Gong, D. Wear 1994, 178, 123.
22. Bahadur, S.; Tabor, D. In Polymer Wear and Its Control; Lee, L. H., Ed.; ACM Symposium Series; Association for Computing Machinery: Washington, DC, 1985; pp 287 and 253.
23. Bahadur, S.; Gong, D.; Anderegg, J. W. Wear 1992, 154, 207.
24. Wang, J.; Gu, M.; Songhao, Ge, S. Wear 2003, 255, 774.
25. Kishore; Sampathkumaran, P.; Seetharamu, S.; Vynatheya, S.; Murali, A.; Kumar, R. K. Wear 2000, 237, 20.
26. Basavarajappa, S.; Chandramohan, G. C. J Mater Sci Tech 2005, 21, 348.
27. Mody, P. B.; Chou, T. W.; Friedrich, K. J Mater Sci 1988, 23, 4319.
28. Smit, B. W. In Engineering Materials Handbook; American Society for Metals: Metals Park, OH, 1997; Vol. 1, p 786.
29. Master, J. E. In Engineering Materials Handbook; American Society for Metals: Metals Park, OH, 1997; Vol. 1, p 781.